IEEE Access
Multidisciplinary | Rapid Review | Open Access Journal

Received April 29, 2019, accepted June 29, 2019, date of publication July 8, 2019, date of current version July 25, 2019.

Digital Object Identifier 10.1109/ACCESS.2019.2927356

3D Visible Light Indoor Positioning by Bokeh Based Optical Intensity Measurement in Smartphone Camera

JOON-WOO LEE, SUNG-JIN KIM, AND SANG-KOOK HAN, (Senior Member, IEEE)
Department of Electrical and Electronic Engineering, Yonsei University, Seoul 03722, South Korea

Corresponding author: Sang-Kook Han (skhan@yonsei.ac.kr)

This work was supported by the Korea Electric Power Corporation under Grant R17XA05-67.

ABSTRACT This paper proposes a three dimensional (3D) high-resolution indoor positioning system that uses a single light-emitting diode (LED) and a complementary metal–oxide semiconductor image sensor (CIS). The proposed visible light positioning system is based on the bokeh effect for improving the positioning accuracy. The 3D position is determined by received signal strength (RSS) and angle of arrival (AOA). Optical saturation in pixels causes severe performance degradation in the RSS-based positioning based on the CIS. The bokeh-based image reception technique resolves this problem by spreading the optical power to adjacent pixels. Additionally, via the bokeh effect, the size of the LED image on the CIS is maintained regardless of the distances. The accuracy of the LED extraction for the AOA can be improved by fixed LED size. These characteristics of the proposed positioning scheme are analyzed via simulations, and the feasibility of the method is verified based on the experimental results. The experimental results indicate an estimated positioning average error rate within 4%.

INDEX TERMS Visible light positioning, CMOS image sensors, light-emitting diodes, image processing.

I. INTRODUCTION

There has been an increased demand for location based services (LBSs) because of the growth of various industries and the development of technology. The most widely used positioning technology is the global positioning system (GPS). However, the accuracy of the GPS is limited to a few meters, and the GPS cannot be applied to indoor environments, because GPS signals are significantly degraded indoors. To overcome the limitations of the GPS for indoor use, radiofrequency (RF) based positioning systems have been widely investigated in recent years, including Bluetooth and Wi-Fi [1]. A high accuracy positioning technique is needed to implement various services, such as finding objects in a market and controlling a robot in a smart factory [2], [3].

The visible light positioning (VLP) technique has attracted research attention because it can be used to implement high accuracy positioning, with advantages, such as robustness to RF interference and low overhead costs. Normally, a photodiode (PD) and a complementary metal–oxide semiconductor image sensor (CIS) are used in the optical receiver for the VLP [4]–[7]. PD based VLP requires an additional PD dongle because there are few smart devices in which PDs are embedded. CIS based positioning has attracted attention because CISs are widely used as built in photo receivers in smartphones [3], [8]–[11].

Most VLP studies focus on indoor positioning. Light-emitting diodes (LEDs) installed in indoor environments are used as anchors to estimate the local positions of devices. In many positioning systems, two or three LEDs are required [3], [8]. However, the use of multiple LEDs negates the advantages gained by using the existing LED infrastructure in VLP systems. Additionally, there are restrictions on the implementation of the VLP technology that is applied for various lighting layouts [8], [12]. For overcoming these restrictions, the demand for single LED based VLP schemes has increased [9], [10]. However, the saturation of the received optical signal in CISs results in the use of additional PDs to measure the received optical power accurately [9].

We propose a high accuracy positioning technique employing a single LED as an anchor and a CIS as a receiver. Two well-known positioning methods are used to implement three dimensional (3D) VLP. The first one involves the received

The associate editor coordinating the review of this manuscript and approving it for publication was Po Yang.

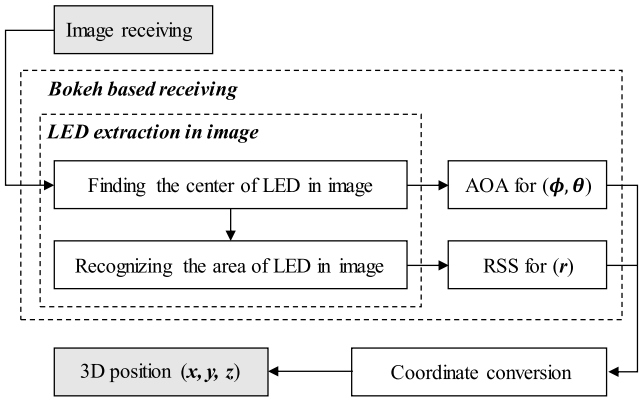

FIGURE 1. Block diagram of the proposed bokeh based 3D positioning.

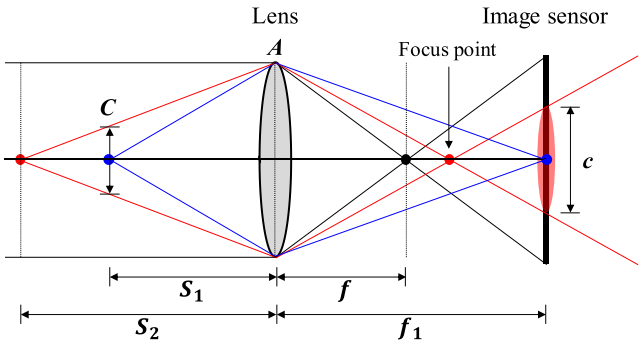

FIGURE 2. Circle of confusion of symmetrical lens.

signal strength (RSS) from the received optical power of the LED. The other involves the angle of arrival (AOA) from the focused LED image on the CIS. Accurately measuring the intensity of the light source is difficult in the CIS based VLP. The saturation of the CIS, which causes the severe degradation of the positioning accuracy, can easily occur when the light source image is captured. The pixels cannot receive an optical power that exceeds the saturation level. Therefore, the measured optical power is lower than the actual one in each pixel.

In this paper, we propose a single LED based high resolution 3D positioning system using a smartphone camera. We can obtain the spherical coordinates of the device from the RSS and AOA. The image blurring condition, i.e., the bokeh effect, is used to enhance the positioning accuracy. This effect improves the RSS accuracy for determining the distance between the LED and the smartphone by preventing optical-power saturation. Additionally, the AOA with the LED extraction process can be simply and accurately implemented, because the size of the focused LED image is fixed via the bokeh effect. We experimentally implemented the single LED based accurate 3D VLP system.

II. SCHEMATICS AND THEORETICAL APPROACH

A block diagram of the proposed visible-light indoor positioning system is shown in Fig. 1. The bokeh-based image receiving has the following special characteristics. 1) The received image is spread via the bokeh effect. 2) The size of the received LED image converges to a specific diameter. These characteristics improve the positioning performance and simplify the positioning process. The proposed method comprises two parts for obtaining the spherical coordinates, i.e., the radial distance (r), polar angle (ϕ), and azimuthal angle (θ). The first part involves determining the AOA, for (ϕ, θ). We must find the center of the LED light in the received image to determine the angles. The proposed method can locate the center of the LED by using two-dimensional (2D) cross-correlation with a same sized reference image because of the second characteristic of the bokeh effect. The second part involves determining the RSS, for (r). We can measure the accurate optical power because the optical saturation is mitigated by the first characteristic. After the center of the LED in the image is located, the area of the LED in the image can be determined according to the center and diameter. The optical power is measured using the area of the LED in the image. Then, the spherical coordinates are converted into rectangular coordinates. The detailed process is described below.

A. USE OF BOKEH EFFECT TO MITIGATE SATURATION IN IMAGE SENSOR

The bokeh effect has been defined as "the way the lens renders out-of-focus points of light." Although image blurring is generally considered as an unwanted effect when taking pictures, it is sometimes intentional for special photo effects. In this study, we received the image using the bokeh effect, intentionally generating an out-of-focus condition to prevent optical power saturation. This effect improved the accuracy of the CIS based light intensity measurement. Before applying the bokeh effect, we verified the factors that determined the features of the bokeh effect in the camera. The lens system of the camera could be approximated by a symmetrical lens, as shown in Fig. 2. The object and image sensor are located on the left and right sides, respectively, of Fig. 2. The distance of the image sensor from the lens is f_1. S_1 is the position of the object when the object image is correctly focused on the image sensor. The position of the focus point, which is the red crossed point on the right side, is short when the object is positioned far from the lens, and the focus point is far from the lens when the object position is short. The minimum distance from the focus point to the lens is f, which is the focal length of the lens. In this case, the object is located at an infinite distance from the lens. The focus point is located between f and the image sensor when the object is located beyond S_1. The object image on the image sensor is convolved by a circle of confusion with diameter c because the focus is not exactly correct at one point [13]. The diameter of the blur circle when the object is positioned at S_2 can be expressed by the following equation:

$$C = \frac{|S_2 - S_1|}{S_2} \cdot A, \tag{1}$$

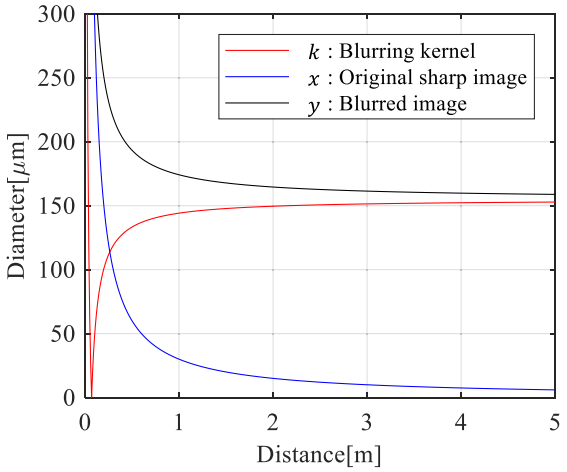

FIGURE 3. Variation of the diameter of the LED and kernel with distance between the LED and camera.

where A is the diameter of the lens, which is expressed as f/N. N is the f-number. The image cast on the image sensor is a circle of diameter c. It can be expressed as

$$c = C \cdot \frac{f_1}{S_1}. \tag{2}$$

The thin lens equation gives

$$f_1 = \frac{f \cdot S_1}{S_1 - f}. \tag{3}$$

Finally, the circle of confusion can be expressed as

$$c = \frac{|S_2 - S_1|}{S_2} \cdot \frac{f^2}{N(S_1 - f)}. \tag{4}$$

The blurred image (y) is determined via the convolution of x and k, where x is the original sharp image and k is the point spread function (blurring kernel). k is the circle of diameter c, and n is the additive noise. y is represented by a linear model [14]:

$$y = k * x + n. \tag{5}$$

In (4), the parameters are all fixed values, except for S_2, which is the distance between the object and the lens. Consequently, S_2 determines the diameter c.

We theoretically verified the variation of the diameter of the LED image and the blur kernel with respect to S_2, as shown in Fig. 3. We used a Samsung Galaxy S8 smartphone as the receiver.

We determined the circle of confusion for this smartphone according to the specifications provided by manufacturer. N was fixed at 1.7 in the rear camera embedded in the smartphone. The value of S_1 was approximately 7 cm when the focus mode was set to the nearest mode. The equivalent focal length (f) of the lens was 26 mm. The value of f was approximately 4.24 mm, considering the actual size of the image sensor. These parameters and S_2 determined c, as shown in Fig. 3.

The foregoing result determined the size of y, and the details are as follows. In this experiment, a single LED (not an array of LEDs) was used as an anchor, and the LED image on the image sensor contained 27 pixels at a 1 m distance when the LED was in-focus. The diameter of x was inversely proportional to the distance between the LED and the camera, as indicated by the plot in Fig. 3. Finally, y could be represented as the convolution of x with k. The diameter of y converged to 160 μm. Considering that the actual size of each pixel was 1.44 μm, the size of the blurred LED image was 111 pixels. We compared these theoretical calculation values with the actual measurement values. We measured the size of the LED at distances ranging from 1 to 4 m, at 1 m intervals. The pixel value of 10 was set as the boundary of the LED area. Although the size of the original LED image decreased as the distance increased, the LED images blurred by the bokeh effect were 110–115 pixels in size, as shown in Fig. 4. Despite the interference factors, such as the interpolation of adjacent pixels, the measured values were similar to the theoretical values. Thus, we theoretically and experimentally verified that the size of the blurred LED image resulting from the intentionally generated bokeh effect was nearly maintained regardless of the distances. The area of the blurred image was several tens of times larger than that of the original LED image, and the light was received in the spread area via the bokeh effect. Thus, the blurred image was more tolerant to saturation than the original image, and we could measure the LED optical power accurately by utilizing the bokeh effect.

B. USE OF BOKEH EFFECT TO EXTRACT LED IMAGE FROM RECEIVED IMAGE

The LED shape and size maintained by the bokeh effect facilitate LED extraction, which involves locating the center of the LED and recognizing the area of the LED in the received image. A solution for determining the position of the LED in the received image is required, because the size of the LED lights changes according to the distance from the image sensor. However, few studies have addressed this process in detail. In the bokeh based LED image reception, we did not consider the changes resulting from the distance, because the size of the LED was maintained at various distances; only the total received optical power was changed. Therefore, 2D cross-correlation is a very simple and powerful solution for locating the center of the LED in the image by using this characteristic of bokeh based reception. First, we set the blurred image obtained using the bokeh effect at a 1 m distance as the reference LED image.

As previously mentioned, the size of the focused image was maintained, and the same reference image was used in 2D cross-correlation to determine the position of the LED in the image. The 2D cross-correlation of an $M \times N$ matrix, X, and a $P \times Q$ matrix, K, is a matrix Y with a size of $(M+P-1) \times (N+Q-1)$ and can be expressed as follows:

$$Y(k,l) = \sum_{m=0}^{M-1} \sum_{n=0}^{N-1} X(m,n)K(m-k, n-l)$$
$$-(P-1) \le k \le M-1, \quad -(Q-1) \le l \le N-1, \tag{6}$$

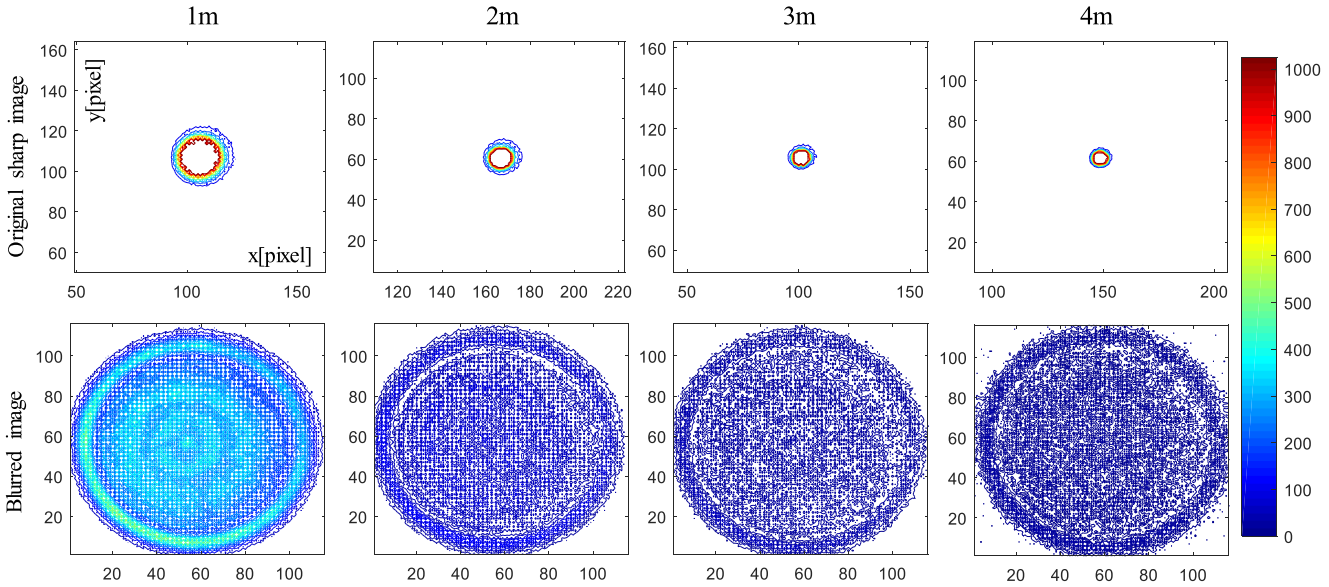

FIGURE 4. Received image in in-focus condition (Original sharp image) and out-of-focus condition (blurred image by bokeh) at various distances.

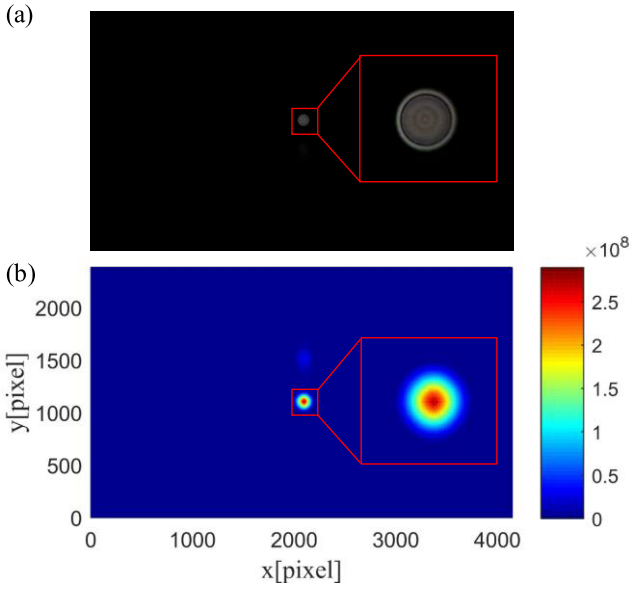

FIGURE 5. (a) Blurred image by bokeh, and (b) result of 2D cross correlation to determine the LED position in the image.

where the matrix K is the reference LED image, and the matrix X is the received LED image in the image sensor. Fig. 5 shows the image of the LED light at a distance of 2 m. Fig. 5(b) presents the result of the 2D cross-correlation, which was used to determine the LED position in the image. The center position of the LED is the point where the maximum value is located in Fig. 5(b). We extracted the LED image with a 115 pixels diameter to measure the optical power.

C. RSS, AOA, AND COORDINATE CONVERSION

We used the RSS and AOA for 3D positioning based on a single LED and camera. The distance (r) was determined according to the RSS. The distance from the LED to the camera was obtained by comparing the received LED optical power with the optical power at 1 m. The optical power was inversely proportional to the square of the distance, and the distance, r, is expressed as

$$r = \sqrt{P_{std}/P}, \tag{7}$$

where the LED optical power at 1 m and the received power are P_{std} and P, respectively [15]. We experimentally verified the distance estimation based on (7). Fig. 6 (a) shows the received optical power of Fig. 4. The sum of the pixels' value in the extracted LED image determines the optical power, and there is no specific unit. Received optical power is smaller in in-focus than out-of-focus because optical saturation clipped the received power in the in-focus condition. We normalized these two conditions based on the optical power of 1 m distance. The black dotted line is theoretical value of optical power that is inversely proportional to the square of the distance. The normalized optical power in out-of-focus is the following blue line and the error was occurred within 10 % compared with the theoretical value. In in-focus condition, the normalized optical power is larger than a few times compared with the theoretical value. Though the above results, we verified that the feasibility of the distance estimation and the process based on bokeh is effective.

The azimuthal angle (ϕ) and the polar angle (θ) were determined according to the incident angle of the LED. The position of the center of the LED image determined these two factors. Fig. 6 shows the spherical coordinates of the LED and the rectangular coordinates of the LED image on the image sensor. The coordinates of the LED image on the image sensor consisted of 2D coordinates on the image sensor (x', y') and the distance between the lens and the image sensor, z'.

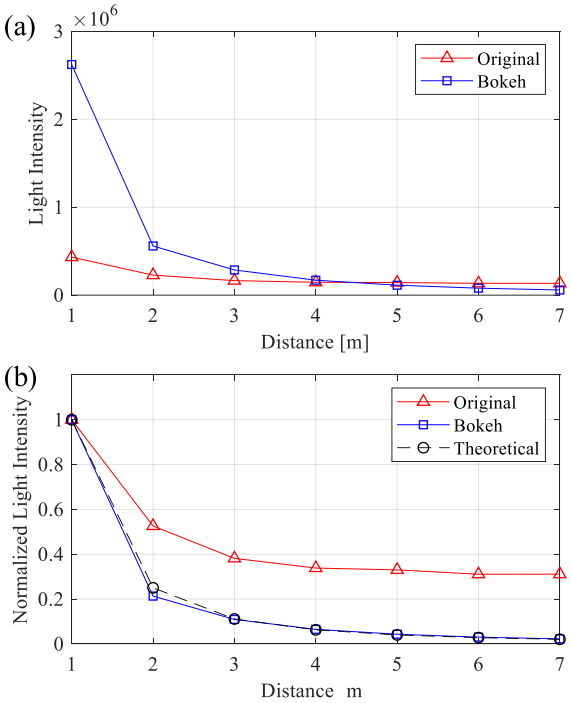

FIGURE 6. (a) Received light intensity at original (in-focus) and bokeh (out-of-focus) conditions. (b) Normalized received light intensity at original, bokeh, and theoretical value.

The coordinates (ϕ, θ) can be expressed by (x', y', z').

$$\phi = \begin{cases} \arctan\left(\frac{x'}{y'}\right), & 0 < x' \\ \arctan\left(\frac{x'}{y'}\right) + 180°, & x' < 0. \end{cases} \tag{8}$$

$$\theta = \arctan\left(\frac{\sqrt{x'^2 + y'^2}}{z'}\right) \tag{9}$$

These spherical coordinates (r, ϕ, θ) were converted into rectangular coordinates (x, y, z) using the following commonly known coordinate transformation formulas. Then, we obtained the 3D rectangular coordinates of the device from the LED.

$$\begin{aligned} x &= r \sin\theta \cos\phi \\ y &= r \sin\theta \sin\phi \\ z &= r \cos\theta \end{aligned} \tag{10}$$

In the local coordinate system (LCS), the position of the LED is denoted as (x, y, z), where the center of the lens is the origin of the LCS. Thus, the real position of the smartphone in a global coordinate system (GCS) can be expressed as (G_x–x, G_y–y, G_z–z), where (G_x, G_y, G_z) represents the position of the LED lights in the GCS.

III. EXPERIMENTAL RESULTS

We used a Samsung Galaxy S8 smartphone to verify the proposed technique. We expect that this positioning scheme is conducted with optical camera communication (OCC) [16]. The exposure time was generally set to a short value, for reducing the inter-symbol interference in the OCC [17]. Additionally, the short exposure times provided the advantage of robustness to optical saturation. For a similar reason, the ISO (an indicator for amplifying the received signal), was set as 100, to avoid optical saturation. A high ISO would interfere with the accurate measurement of the received optical power because it would introduce noise in the image [17]. The raw image was used to mitigate the optical power distortion that occurred in the image signal processor.

We experimentally verified the proposed scheme under the assumption that the reference values were transmitted via OCC. The LED optical power at 1 m was necessary for determining the distance according to (7). Additionally, the coordinates of the LED in the GCS were needed to

TABLE 1. Camera options and experimental parameters.

PARAMETER	VALUE
Phone model	Samsung Galaxy S8
Field of view (FoV)	40°
Exposure time	1/24000 s
ISO	100
Diameter of LED light	~5 mm
Image resolution	4032 × 3024 (raw image)
Pixel size	1.44 μm
Focus mode	Near (~7 cm)

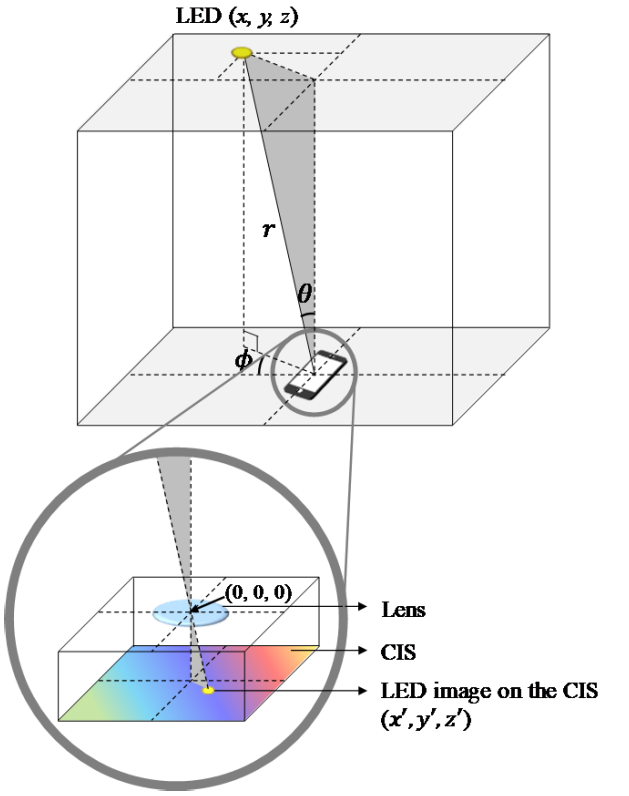

FIGURE 7. Local coordinates system with the LED and the LED image on the image sensor.

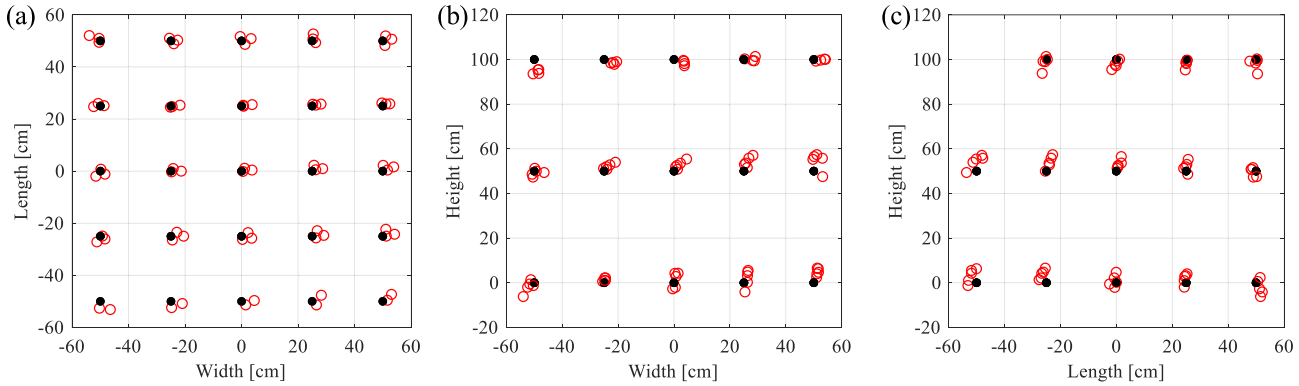

FIGURE 8. Positioning results for 64 positions without rotation at (a) X-Y, (b) X-Z, and (c) Y-Z surfaces.

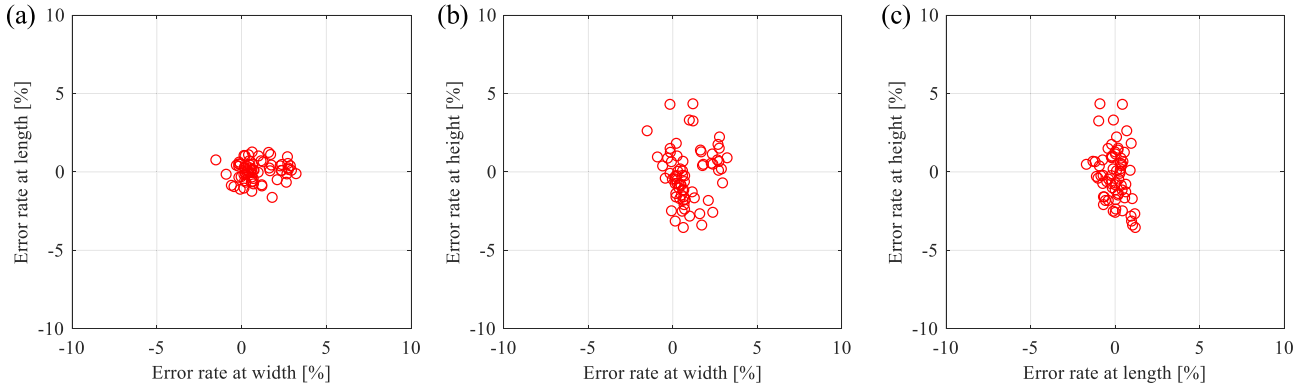

FIGURE 9. The error rate for various 70 points without rotation at (a) X-Y, (b) X-Z, and (c) Y-Z surfaces.

obtain the real coordinates of the device. We expect that the LED transmitted these two reference values using OCC, as reported in our previous work [16]. The Manchester-encoded signal of the LED added a stripe pattern in the bokeh image, attenuating the received optical power. This encoded signal had an equivalent ratio of 1(on)-0(off), and the optical power was nearly half of that in the case where no signal was added to the LED. Thus, we must consider the received optical power attenuation when we transmit these reference values via the LED.

We estimated 70 different positions using the proposed positioning scheme to evaluate its performance. We verified the proposed positioning system in a 1 m × 1 m × 2.4 m space. We mounted LED lights on the ceiling, and the position of the LED lights was denoted in the GCS as (0, 0, 240 cm). In this condition, we shifted the position of the smartphone with no rotation. The smartphone was placed at 25 positions, at heights of 0 and 0.5 m. There were only 20 positions at a height of 1 m owing to the limitation of the camera FoV. These 70 points are shown in Fig. 8. The results indicate the actual and estimated positions for the *X-Y*, *X-Z*, and *Y-Z* surfaces. The black points and red rings represent the actual and estimated positions, respectively.

The positioning error was proportional to the distance between the LED and the camera, as indicated by (10). Thus, we expressed the error rate as the ratio of the error to the distance in Fig. 9. We defined the positioning error rate (PER) as

$$PER(\%) = \frac{\sqrt{\Delta x^2 + \Delta y^2 + \Delta z^2}}{\sqrt{x^2 + y^2 + z^2}} \times 100, \tag{11}$$

where Δx, Δy, and Δz are the errors (differences between the estimated and actual values) of x, y, and z, respectively. Therefore, we expressed the positioning performance as the ratio of the error to the distance, as shown in Fig. 9. The average ratio was 2.09 %, and the maximum ratio was 4.56 %. These results indicate the feasibility of the proposed scheme based on single LED based 3D positioning.

In a realistic condition, the smartphone rotates about various axes. This rotation causes additional error. To quantify the error due to rotation, we investigated 64 cases where the smartphone rotated at various angles and applied a rotation-compensation technique based on the rotation matrix from Euler's theorem [18]. The Android platform included a geomagnetic field sensor and an accelerometer for determining the position of the device. The pitch (ψ_x), roll (ψ_y), and azimuth (ψ_z) angles were provided by these sensors. The pitch was defined as the angle between a plane parallel to the screen of the device and a plane parallel to the ground. The roll was perpendicular to the pitch. The azimuth was the

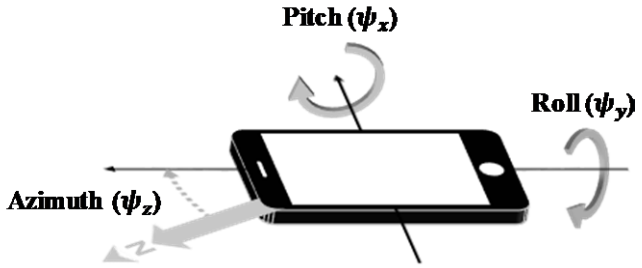

FIGURE 10. The azimuth, pitch and roll of the smartphone.

angle between the current compass direction of the device and magnetic north. Theses angles are presented in Fig. 10. We derived the rotation matrix based on Euler's theorem. The rotation matrix $\boldsymbol{R}$ is expressed as

$$\boldsymbol{R} = \boldsymbol{R}_z\boldsymbol{R}_x\boldsymbol{R}_y = \begin{bmatrix} \cos\psi_z & \sin\psi_z & 0 \\ \sin\psi_z & \cos\psi_z & 0 \\ 0 & 0 & 1 \end{bmatrix} \times \begin{bmatrix} 1 & 0 & 0 \\ 0 & \cos\psi_x & \sin\psi_x \\ 0 & -\sin\psi_x & \cos\psi_x \end{bmatrix} \times \begin{bmatrix} \cos\psi_y & 0 & \sin\psi_y \\ 0 & 1 & 0 \\ -\sin\psi_y & 0 & \cos\psi_y \end{bmatrix} \quad (12)$$

When the smartphone rotated by ψ_x, ψ_y, and ψ_z, (x, y, z) was transformed into $(\hat{x}, \hat{y}, \hat{z})$, which can be expressed as

$$\begin{bmatrix} \hat{x} \\ \hat{y} \\ \hat{z} \end{bmatrix} = \boldsymbol{R}[x \quad y \quad z]^T. \quad (13)$$

We could compensate for the rotation error because we knew the relationship between before and after the rotation, as indicated by (13).

We experimentally verified the rotation compensation based on the rotation matrix. We fixed the smartphone at (0, 0, 0), and the LED at (0, 0, 240 cm). To verify the error due to rotation, we rotated the smartphone as follows: $\psi_x \in (-23°, 25°)$, $\psi_x \in (-17°, 18°)$, and $\psi_z \in (-9°, 21°)$. The pitch and roll were close to the maximum rotation angle, within the limitation of the FOV. Although the smartphone was fixed at (0, 0, 0), the images of the LED lights were shifted to various positions on the image sensor via rotation. The positioning results without rotation compensation included the error due to rotation, as shown in Fig. 11. Here, the blue circles represent the positioning results without rotation compensation. After the rotation compensation, the blue circles transformed into the red circles, and Fig. 12 shows the error rate of the compensation results. The average and maximum error rates were 1.39% and 3.14%, respectively.

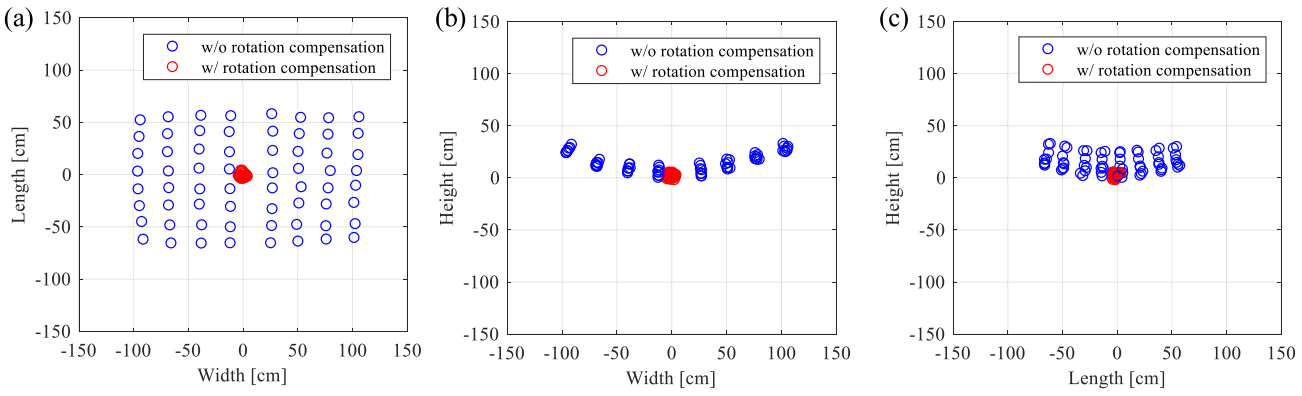

FIGURE 11. Positioning results for various rotation of 64 cases at (a) X-Y, (b) X-Z, and (c) Y-Z surfaces.

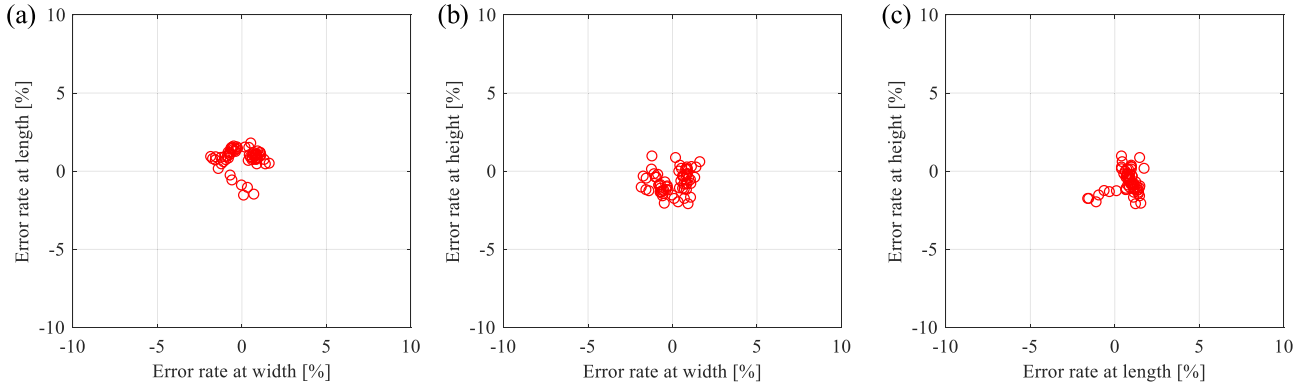

FIGURE 12. The error rate for various rotation of 64 cases after rotation compensation at (a) X-Y, (b) X-Z, and (c) Y-Z surfaces.

It is considered that the measurement error caused by the embedded sensors accounted for a large proportion of the total error. Thus, this error was added to the positioning results of Figs. 8 and 9.

The total error rate was estimated by considering the changes of the position and angle. In the first scenario, the smartphone was moved to 70 points without rotation, as shown in Fig. 9. The second scenario involved 64 cases of rotating angles at a fixed point, as shown in Fig. 12. Error measurement while simultaneously changing the position and angle of the smartphone is an ideal method, but the number of measurement cases increases exponentially. For convenience, we separately measured the error for these two scenarios. Consequently, the proposed positioning scheme had an average error rate of 3.48 %.

The error included the performance-degradation factors, such as the angle gain and lens distortion. We can predict the performance enhancement by considering these factors, but we did not address these issues in the present study. This experimental results indicate that the error was <10 cm when the height of the LED was 2.4 m. We expect that the proposed scheme may be feasible in applications such as indoor LBSs and for controlling robots in smart factories.

IV. CONCLUSION

We proposed a single LED based 3D positioning system based on a CIS. Spherical coordinates were obtained using the RSS and AOA. The receiver could receive an accurate optical power through the bokeh effect, which fundamentally prevents optical power saturation. Further, we were easily able to extract the LED image from the received image with a reasonable LED image size regardless of the distance between the transmitter and receiver. We achieved this by using the bokeh effect. We experimentally implemented the single LED and CIS based VLP, and the average error was 3.48%. The results indicate that the proposed indoor positioning technique is effective for indoor LBSs that use existing lighting and receiver infrastructure.

REFERENCES

[1] H. Liu, H. Darabi, P. Banerjee, and J. Liu, "Survey of wireless indoor positioning techniques and systems," *IEEE Trans. Syst., Man, Cybern. C, Appl. Rev.*, vol. 37, no. 6, pp. 1067–1080, Nov. 2007.
[2] A. Jovicic, J. Li, and T. Richardson, "Visible light communication: Opportunities, challenges and the path to market," *IEEE Commun. Mag.*, vol. 51, no. 12, pp. 26–32, Dec. 2013.
[3] J.-Y. Kim, S.-H. Yang, Y.-H. Son, and S.-K. Han, "High-resolution indoor positioning using light emitting diode visible light and camera image sensor," *IET Optoelectron.*, vol. 10., no. 5, pp. 184–192, 2016.
[4] S. H. Yang, E. M. Jeong, and S. K. Han, "Indoor positioning based on received optical power difference by angle of arrival," *Electron. Lett.*, vol. 50, no. 1, pp. 49–51, Jan. 2014.
[5] S. H. Yang, H. S. Kim, Y. H. Son, and S. K. Han, "Three-dimensional visible light indoor localization using AOA and RSS with multiple optical receivers," *J. Lightw. Technol.*, vol. 32, no. 14, pp. 2480–2485, Jul. 15, 2014.
[6] H. Zheng, Z. Xu, C. Yu, and M. Gurusamy, "A 3-D high accuracy positioning system based on visible light communication with novel positioning algorithm," *Opt. Commun.*, vol. 396, pp. 160–168, Aug. 2017.
[7] T.-H. Do and M. Yoo, "An in-depth survey of visible light communication based positioning systems," *Sensors*, vol. 16, no. 5, p. 678, 2016.
[8] L. Li, P. Hu, and C. Peng, "Epsilon: A visible light based positioning system," in *Proc. NSDI*, 2014, pp. 331–343.
[9] Y. Hou, Y. Xue, C. Chen, and S. Xiao, "A RSS/AOA based indoor positioning system with a single LED lamp," in *Proc. Int. Conf. Wireless Commun. Signal Process. (WCSP)*, Oct. 2015, pp. 1–4.
[10] R. Zhang, W.-D. Zhong, Q. Kemao, and S. Zhang, "A single LED positioning system based on circle projection," *IEEE Photon. J.*, vol. 9, no. 4, Aug. 2017, Art. no. 7905209.
[11] T.-H. Do and M. Yoo, "Visible light communication based vehicle positioning using LED street light and rolling shutter CMOS sensors," *Opt. Commun.*, vol. 407, pp. 112–126, Jan. 2018.
[12] W. Pan, Y. Hou, and S. Xiao, "Visible light indoor positioning based on camera with specular reflection cancellation," in *Proc. Conf. Lasers Electro-Opt. Pacific Rim (CLEO-PR)*, Jul./Aug. 2017, pp. 1–4.
[13] H. M. Merklinger, "A different approach—The object field," in *The Ins and Outs of Focus*. Internet Edition, 2002, pp. 25–58. [Online]. Available: http://www.trenholm.org/hmmerk/download.html
[14] P. Vivirito, S. Battiato, S. Curti, M. La Cascia, and R. Pirrone, "Restoration of out-of-focus images based on circle of confusion estimate," *Proc. SPIE*, vol. 4790, pp. 408–417, Nov. 2002.
[15] J. M. Kahn and J. R. Barry, "Wireless infrared communications," *Proc. IEEE*, vol. 85, no. 2, pp. 265–298, Feb. 1997.
[16] J.-W. Lee, S.-J. Kim, and S.-K. Han, "Adaptive window thresholding for noise-robust photo detection in OCC," *Opt. Commun.*, vol. 426, pp. 623–628, Nov. 2018.
[17] T.-H. Do and M. Yoo, "Performance analysis of visible light communication using CMOS sensors," *Sensors*, vol. 16, no. 3, p. 309, 2016.
[18] A. Poulose, O. S. Eyobu, and D. S. Han, "An indoor position-estimation algorithm using smartphone IMU sensor data," *IEEE Access*, vol. 7, pp. 11165–11177, 2019.

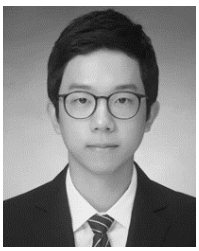

JOON-WOO LEE received the B.S. degree in electrical and electronic engineering from Ajou University, Suwon, South Korea, in 2015. He is currently pursuing the Ph.D. degree in electrical and electronic engineering with Yonsei University. His current research interests include visible-light communication, optical camera communication, and indoor positioning systems.

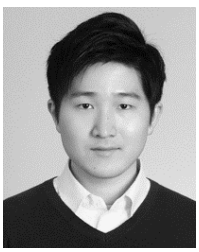

SUNG-JIN KIM received the B.S. degree in electrical and electronic engineering from Yonsei University, Seoul, South Korea, in 2013, where he is currently pursuing the Ph.D. degree in electrical and electronic engineering. His current research interests include visible-light communication, optical camera communication, optical MIMO, and optical systems for communications.

SANG-KOOK HAN received the B.S. degree in electronic engineering from Yonsei University, Seoul, South Korea, in 1986, and the M.S. and Ph.D. degrees in electrical engineering from the University of Florida, Gainesville, FL, USA, in 1994. From 1994 to 1996, he was with the System IC Laboratory, Hyundai Electronics, where he was involved in the development of optical devices for telecommunications. He is currently a Professor with the Department of Electrical and Electronic Engineering, Yonsei University. His current research interests include optical devices/systems for communications, optical OFDM transmission system, passive optical networks, optical networks, and visible-light communication technologies.